Spiroconjugation. The Electronic Spectrum of a Spirotetrene

R. Boschi,[1a] A. S. Dreiding,[1b] and E. Heilbronner[1a]

Contribution from the Institute of Physical Chemistry, University of Basel, Basel, and of the Institute of Organic Chemistry, University of Zürich, Zürich, Switzerland.
Received June 2, 1969

Abstract: Spiroconjugation in spiro[5.5]undeca-1,4,6,9-tetraene-3,8-dione (I) leads to a bathochromic shift of -7400 cm^{-1} of the high-energy absorption band ($\pi^* \leftarrow \pi$ transition ($B_2 \leftarrow A_1$ (D_{2d})) at 50,000 cm^{-1}) as compared to the corresponding band in the spectrum of the cross-conjugated dienone spiro[5.5]undeca-1,4-dien-3-one ($\pi^* \leftarrow \pi$ transition ($A_1 \leftarrow A_1$ (C_{2v})) at 57,000 cm^{-1}). The long-wavelength bands ($\pi^* \leftarrow$ n at 29,000 cm^{-1}; $\pi^* \leftarrow \pi$ at 43,000 cm^{-1}) are insensitive to spiroconjugation. This result is in agreement with the predictions derived from the molecular orbital model proposed by Simmons and Fukunaga and by Hoffmann, Imamura, and Zeiss which describes spiroconjugation as mainly due to electron delocalization.

The phenomenon of spiroconjugation has been examined by Simmons and Fukunaga[2a] and by Hoffmann, Imamura, and Zeiss[2] on the basis of the Hückel molecular orbital approximation. The contribution of exciton delocalization toward the changes which occur in the electronic spectrum, when two subsystems are spiroconnected, has also been considered by Simmons and Fukunaga (Simpson's "independent system approach"[3]).

A more detailed analysis of the electron-spectroscopic consequences of spiroconjugation, including effects due to electron–electron repulsion, had previously been worked out by Hohlneicher,[4] but his results were—at the time—unfortunately not generally available.

In this note we wish to report on the electronic spectrum of spiro[5.5]undeca-1,4,6,9-tetraene-3,8-dione (I), a member of the class of compounds named "spirotetrenes" by Farges and Dreiding.[5] As a reference we are using the electronic spectrum of the dienone chromophore present in spiro[5.5]undeca-1,4-dien-3-one (II).[6]

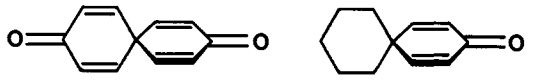

I II

Electronic Spectra

The electronic spectra of I and II shown in this paper have been recorded on a McPherson double-beam spectrometer (Model 225) from *n*-hexane solutions (path lengths 1.0 mm). The original data were fed to a CDC 1604 digital computer and the smoothed absorption curves plotted. Figures 1 and 2 are reproductions of the computer drawn curves.

Table I. Characteristic Values of the Electronic Spectra of I and II[a]

Band	I $\tilde{\nu}$, cm^{-1}	I λ, nm	I log ϵ, l. mol^{-1} cm^{-1}	II $\tilde{\nu}$, cm^{-1}	II λ, nm	II log ϵ, l. mol^{-1} cm^{-1}
d	50,000	200	4.71	57,400	174	4.52
c	44,000	228	4.34	42,900	233	4.25
a						
$m = 9$				33,400	299	0.39
8				32,300	310	0.63
7	32,000	313	1.36	31,000	322	1.00
6	30,800	325	1.44	29,900	335	1.19
5	29,600	338	1.47	28,700	349	1.27
4	28,500	352	1.45	27,600	362	1.21
3	27,400	366	1.32	26,500	377	1.00
2	26,200	382	0.98	25,600	391	0.68
1	25,100	398	0.40			

[a] The solvent was *n*-hexane (room temperature). All $\tilde{\nu}$ values have been rounded to the nearest 100 cm^{-1}. Indices *m* refer to the fine structure maxima of the a bands.

The numbering of the bands and band features, as indicated in Figures 1 and 2, is arbitrary and serves only in referring to the data given in Table II. The inserts (ϵ *vs.* $\tilde{\nu}$) yield a more detailed insight into the fine structure of the $\pi^* \leftarrow$ n bands. The progression of the fine structure maxima in the $\pi^* \leftarrow$ n bands can be represented by

$$\tilde{\nu}_a(m) = 23915 + 1149m \text{ (cm}^{-1}\text{)} \quad (I)$$

$$r = 0.99984$$

$$\tilde{\nu}_a(m) = 23165 + 1130m \text{ (cm}^{-1}\text{)} \quad (II)$$

$$r = 0.99929$$

(1) (a) University of Basel; (b) University of Zürich.
(2) (a) H. E. Simmons and T. Fukunaga, *J. Amer. Chem. Soc.*, **89**, 5208 (1967); (b) R. Hoffmann, A. Imamura, and G. D. Zeiss, *ibid.*, **89**, 5215 (1967).
(3) W. T. Simpson, "Theories of Electrons in Molecules," Prentice-Hall, Englewood Cliffs, N. J., 1962, p 141.
(4) G. Hohlneicher, Habilitationsschrift, Technische Hochschule, München, 1967.
(5) G. Farges and A. S. Dreiding, *Helv. Chim. Acta*, **49**, 552 (1966).
(6) R. Burnell and W. I. Taylor, *J. Chem. Soc.*, 3486 (1954); A. S. Dreiding, *Helv. Chim. Acta*, **40**, 1812 (1957).

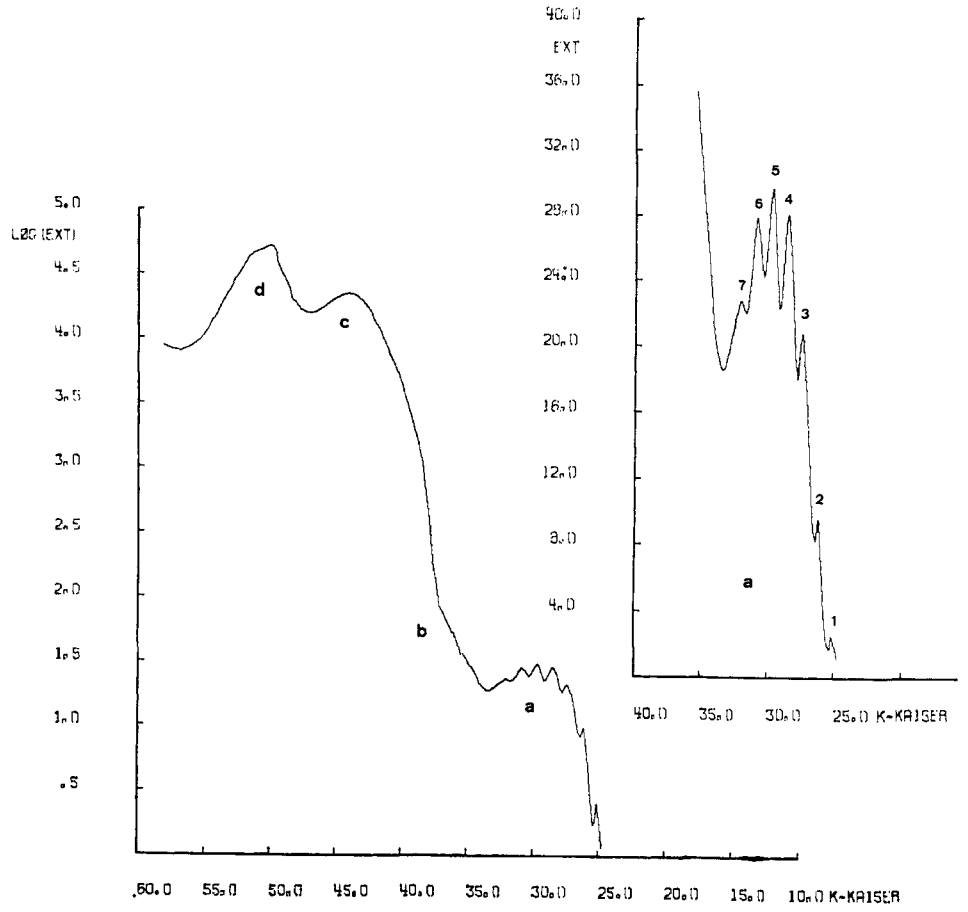

Figure 1. Electronic spectrum of spiro[5.5]undeca-1,4,6,9-tetraene-3,8-dione (I).

where m is the index of the particular fine structure maximum and r is the correlation coefficient.

Ethanolic solutions of I and II yield electronic spectra in which the bands labeled c are bathochromically displaced (I, $\Delta\bar{\nu} = -1100$ cm^{-1}; II, $\Delta\bar{\nu} = -1600$ cm^{-1}) while the a bands are shifted toward higher wave numbers by about $\Delta\bar{\nu} \approx 1000$ to 2000 cm^{-1}. This value cannot be determined exactly, because in ethanolic solution the $\pi^* \leftarrow$ n bands lose their fine structure completely. Let us consider what predictions can be de-

Table II. Praiser–Parr–Pople CI Treatment of the Dienone III and the Spirotetrenedione I[a,b]

	eV	$\bar{\nu}_{calcd}$	$\bar{\nu}_{exp}$[c]	f_{calcd}	log ε exptl[c]	Irred repr	Pol	Dominating config
				Dienone III				
E_0						A_1		Γ, 0.96
E_1	4.377	35,300		0.1		B_2	y	$\psi_2^{-1}\psi_{-1}$, 0.99
E_2	5.230	42,200	42,900	0.6	4.25	A_1	z	$\psi_1^{-1}\psi_{-1}$, 0.85
E_3	6.346	51,200		0.01		B_2	y	$\psi_1^{-1}\psi_{-2}$, 0.99
E_4	7.337	59,200		0.04		A_1	z	$\psi_3^{-1}\psi_{-1}$, 0.80
E_5	7.456	60,100	57,400	1.1	4.52	A_1	z	$\psi_2^{-1}\psi_{-2}$, 0.83
E_6	8.506	68,600		0.1		A_1	z	$\psi_1^{-1}\psi_{-3}$, 0.93
				Spiro Compound I				
E_0						A_1		Γ, 0.95
E_1	4.128	33,300		0.04		E	x,y	$\psi_3^{-1}\psi_{-2}$; $\psi_3^{-1}\psi_{-1}$, 1.00
E_2	5.045	40,700	44,000	1.9	4.34	B_2	z	$1/\sqrt{2}(\psi_2^{-1}\psi_{-1} - \psi_1^{-1}\psi_{-2})$, 0.94
E_3	5.407	43,600		0.0		A_1, A_2	forbd	$\psi_1^{-1}\psi_{-1}$; $\psi_2^{-1}\psi_{-2}$, 0.97
E_4	6.100	49,200		0.0		E	x,y	$\psi_1^{-1}\psi_3$; $\psi_3^{-1}\psi_{-3}$, 1.00
E_5	6.519	52,600	50,000	2.3	4.71	B_2	z	$\psi_3^{-1}\psi_{-3}$, 0.98
E_6	6.560	52,900		0.0		B_1	forbd	$1/\sqrt{2}(\psi_2^{-1}\psi_{-1} + \psi_1^{-1}\psi_{-2})$, 0.92

[a] See Appendix for assumptions and parameters. [b] E_j = energy of state Ψ_j relative to the energy $E_0 = 0$ of the ground state Ψ_0. Pol = direction of polarization, the z axis being the twofold axis of III or the S_4 axis of I. The number beside the dominating configuration $\psi_j^{-1}\psi_k$ is the coefficient in the linear combination Ψ_j. f_{calcd} = computed oscillator strength. [c] These values refer to compound II.

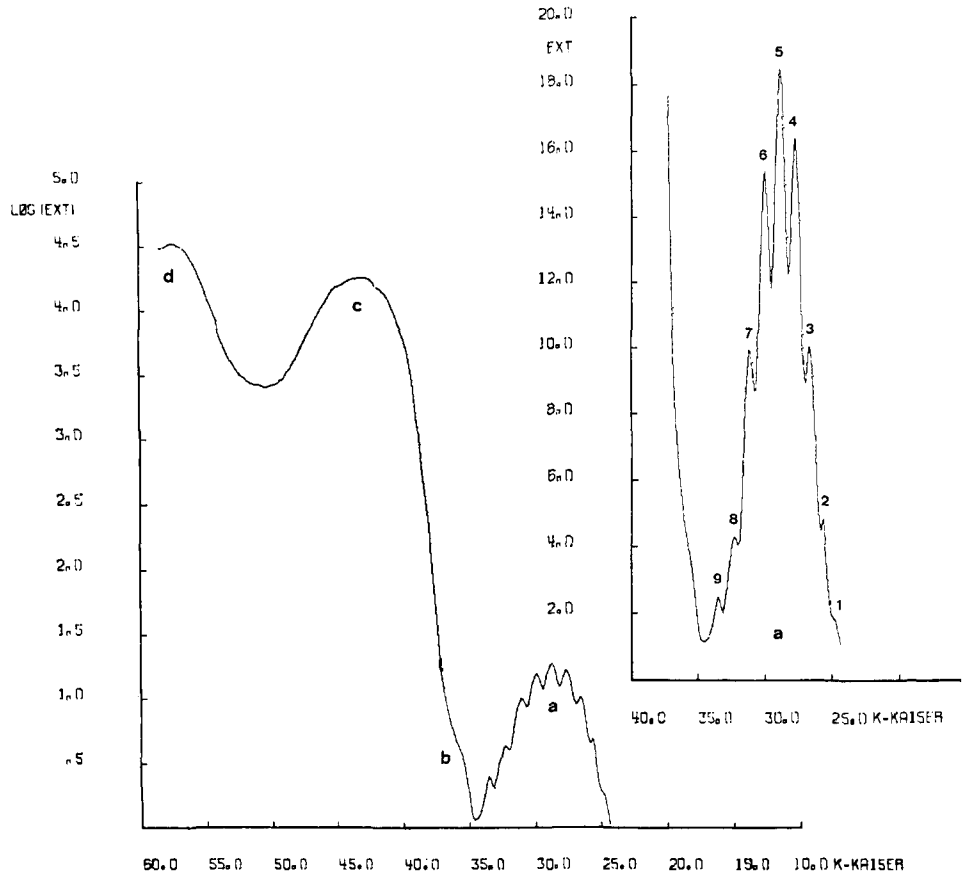

Figure 2. Electronic spectrum of spiro[5.5]undeca-1,4-diene-3-one (II).

rived from the orbital scheme proposed by Simmons, Hoffmann, and their coworkers[2a,b] concerning the relative spectroscopic behavior of I and II.

Reference Compound II

In the following we shall assume that the dienone chromophore present in II has C_{2v} symmetry. Using the recommended value of $\alpha_O = \alpha + \beta$ for the oxygen atomic orbital Coulomb integral[7] and setting all resonance integrals between bonded centers equal to β, one obtains six HMO's for the dienone π system III (see Figure 3), the four inner orbitals of which are shown in the diagram of Figure 3. They belong to the following irreducible representations of the group C_{2v}: $\psi_2(A_2) = a_2$; $\psi_3(B_1) = b_1$; $\psi_4(B_1) = b_1^*$; $\psi_5(A_2) = a_2^*$. Due to the particular choice of $\alpha_O = \alpha + \beta$, the orbitals a_2 and b_1 are accidentally degenerate: $\epsilon(a_2) = \epsilon(b_1) = \alpha + \beta$. Apart from the ground configuration $\Gamma(A_1)$ to which we assign the energy zero, we shall consider only the four singly excited configurations of the dienone π system.

Configuration	Representation	Polarization	Energy
Γ	A_1		0
$\Psi(b_1^* \leftarrow b_1)$	A_1	z	-1.254β
$\Psi(b_1^* \leftarrow a_2)$	B_2	y	-1.254β
$\Psi(a_2^* \leftarrow b_1)$	B_2	y	-2.000β
$\Psi(a_2^* \leftarrow a_2)$	A_1	z	-2.000β

(1)

Electronic transitions from Γ to configurations belonging to A_1 (B_2) are polarized parallel to the z (y) axis. Two corrections, which in our model affect the order and relative spacing of the orbitals and hence of the configurations, have to be considered: (a) small deviations $\delta\alpha_O$ from the Coulomb integral α_O assumed in the above calculations; (b) changes $\delta\beta$ in the resonance integrals $\beta_{\mu\nu}$ of the π bonds, which account for the bond localization which must necessarily exist in a π system such as III. To simplify matters we shall assume a value of $\beta + \delta\beta$ for the localized π bonds 1–2, 3–4, 5–6, and $\beta - \delta\beta$ for the nonessential π bonds 2–3 and 2–5.

Corrections a and b yield to first order the following changes in the energies $E(\Psi_j)$ of the configurations Ψ_j of our simple model.

$$\begin{aligned} E(b_1^* \leftarrow b_1) &= -1.254\beta + 0.344\alpha_O - 1.444\delta\beta \\ E(b_1^* \leftarrow a_2) &= -1.254\beta - 0.156\alpha_O - 1.944\delta\beta \\ E(a_2^* \leftarrow b_1) &= -2.000\beta + 0.500\alpha_O - 1.500\delta\beta \\ E(a_2^* \leftarrow a_2) &= -2.000\beta \qquad\qquad - 2.000\delta\beta \end{aligned} \tag{2}$$

In particular, choosing $\delta\beta = 0.2\beta$ as a conservative estimate for the effect of bond localization to be expected in the system III, we obtain

$$\begin{aligned} E(b_1^* \leftarrow b_1) &= -1.543\beta + 0.344\delta\alpha_O \\ E(b_1^* \leftarrow a_2) &= -1.643\beta - 0.156\delta\alpha_O \\ E(a_2^* \leftarrow b_1) &= -2.300\beta + 0.500\delta\alpha_O \\ E(a_1^* \leftarrow a_2) &= -2.400\beta \end{aligned} \tag{3}$$

Note that depending on the sign and magnitude of $\delta\alpha_O$, the energies of the pairs of configurations of low

(7) A. Streitwieser, Jr., "Molecular Orbital Theory for Organic Chemists," John Wiley & Sons, Inc., New York, N. Y., 1961.

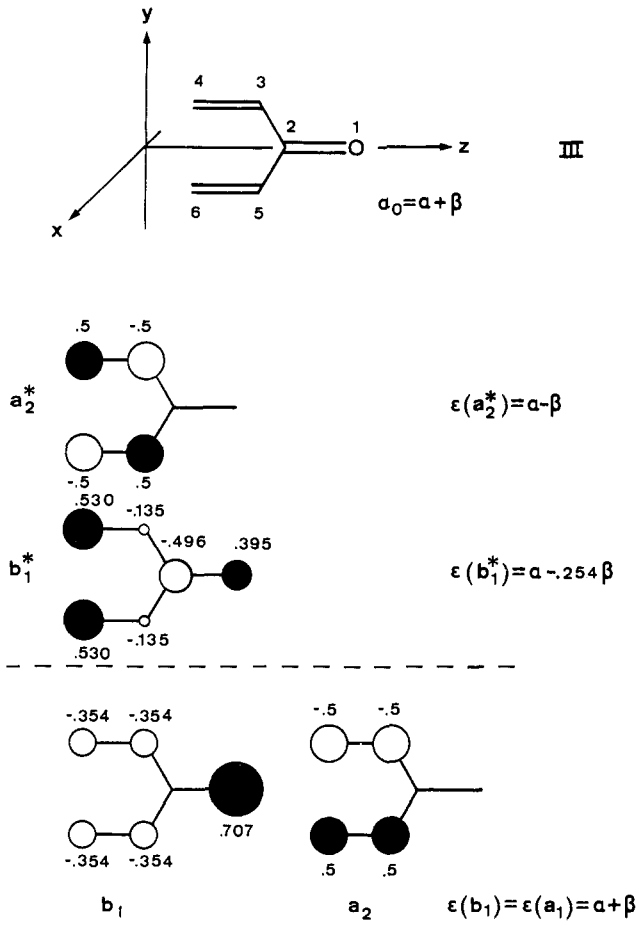

Figure 3. Inner molecular π orbitals of a cross-conjugated dienone (III).

or high energy may again be made to coincide. This means that in view of the crudeness of our model and of the intensity relationships to be discussed below, we shall not be able to predict the positions of the weak transitions relative to the intense ones which occur in the same wave number region.

An estimate of the relative intensities of the bands corresponding to the transitions from Γ to one of the excited configurations is obtained by squaring the transition integrals

$$\langle\psi_J|z|\psi_K\rangle \approx \sum_\mu c_{J\mu}c_{K\mu}z_\mu \quad (A_1)$$
$$\langle\psi_J|y|\psi_K\rangle \approx \sum_\mu c_{J\mu}c_{K\mu}y_\mu \quad (B_2) \qquad (4)$$

depending on the irreducible representation to which the excited configuration belongs.

For $\alpha_O = \alpha + \beta$ ($\delta\alpha_O = 0$) and $\delta\beta = 0$ we obtain for the C_{2v} conformation of III the values given below (5) if all bond angles are assumed to be 120° and all bonds of equal length (in the values quoted the bond length is used as a unit). The effect of bond localization on the transition intensities can be visualized by considering the extreme case of "complete localization" where the bonds 1–2, 3–4, and 5–6 are pure double bonds and the bonds 2–3 and 2–5 are ineffective.

$$\alpha_O = \alpha + \beta(\delta\alpha_O = 0,\ \delta\beta = 0)$$

		Completely localized bonds
$(\langle b_1^*\|z\|b_1\rangle)^2$	$= (0.794)^2 = 0.63$	$\longrightarrow 0.20$
$(\langle b_1^*\|y\|a_2\rangle)^2$	$= (0.342)^2 = 0.12$	$\longrightarrow 0.00$
$(\langle a_2^*\|y\|b_1\rangle)^2$	$= (0.000)^2 = 0.00$	$\longrightarrow 0.00$
$(\langle a_2^*\|z\|a_2\rangle)^2$	$= (0.500)^2 = 0.25$	$\longrightarrow 0.25$

(5)

If we disregard deviations from the Coulomb integral $\alpha_O = \alpha + \beta$, we obtain with $\beta = -24{,}000$ cm^{-1} from (3) the following predictions for the strong $\pi^* \leftarrow \pi$ bands in the electronic spectrum of the dienone system III: $E(b_1^* \leftarrow b_1) = 37{,}000$ cm^{-1} and $E(a_2^* \leftarrow a_2) = 58{,}000$ cm^{-1}. This is in reasonable agreement with the observed spectrum of II (see Figure 2). As can be deduced from (5), the intensities of these two strong bands are predicted to be of roughly equal magnitude for an intermediate amount of bond localization. The two weak bands predicted to occur in the same regions are obliterated by the more intense ones and hence escape observation. It could be argued that the low intensity shoulder observed on the long wave end of the first $\pi^* \leftarrow \pi$ band belongs to the $b_1^* \leftarrow a_2$ transition. This would be in agreement with deductions based on the photochemistry of dienones.[8]

The $\pi^* \leftarrow \pi$ bands are preceded by a fine-structured $\pi^* \leftarrow$ n band with maximum at about 29,000 cm^{-1}. Based on this value, the level of the lone-pair orbital n has to be adjusted to $\epsilon(n) = \alpha + 0.75\beta$ to fit the observed position of the $b_1^* \leftarrow$ n transition, if the value $\delta\beta = 0.2\beta$ is used as indicated above to correct the orbital energy $\epsilon(b_1^*)$ for bond localization.

Spiro Compound I

We shall assume that I is present in solution in an idealized conformation of D_{2d} symmetry. (Dreiding models indicate that the favored conformations of I are chiral and of C_2 symmetry only. However, the deviations from D_{2d} are presumably small enough to be irrelevant for our argument.)

Treating the spiroconjugation between the two dienone subsystems in I as a first-order interaction between pairs of degenerate orbitals of the two subsystems, as shown in ref 1 and 2, we obtain

Subsystems II (left) C_{2v}	+	II (right) C_{2v}	Spirosystem I D_{2d}
			$\cdot a_2^*$
a_2^*	±	a_2^*	
			$\cdot b_1^*$
b_1^*	±	b_1^*	$\cdot e^*$
b_1	±	b_1	$\cdot e$
			$\cdot a_2$
a_2	±	a_2	
			$\cdot b_1$

(6)

The orbitals $\cdot e$ and $\cdot e^*$ are degenerate pairs belonging to the irreducible representation $\cdot E$ of D_{2d}, while $\cdot a_2$ and $\cdot a_2^*$ and $\cdot b_1$ and $\cdot b_1^*$ belong to $\cdot A_1$ and $\cdot B_1$, respectively (a dot has been used to distinguish the orbitals belonging to irreducible representations of D_{2d} from those of C_{2v} carrying the same symbols).

From the Newman projections given it is immediately apparent that the linear combinations of a_2 or a_2^* orbitals belonging to $\cdot B_1$ are bonding and those

(8) H. E. Zimmerman and J. S. Swenton, *J. Amer. Chem. Soc.*, **86**, 1436 (1964); N. J. Turro, "Molecular Photochemistry," W. A. Benjamin Inc., New York, N. Y., Amsterdam, 1965, p 162.

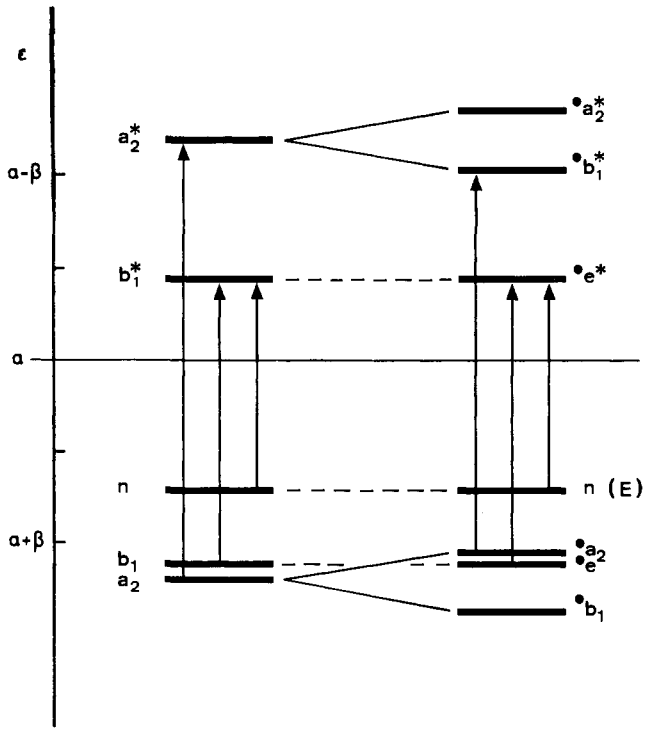

Figure 4. Orbital correlation diagram for the inner orbitals of the dienone subsystems III (left) and of the spiroconjugated system I (right). The vertical arrows refer to only those transitions which give rise to the three observable bands in the spectra of I and II.

belonging to $\cdot A_2$ antibonding, with respect to the orbital energies of the separated orbitals a_1 or a_2^*. It is easy

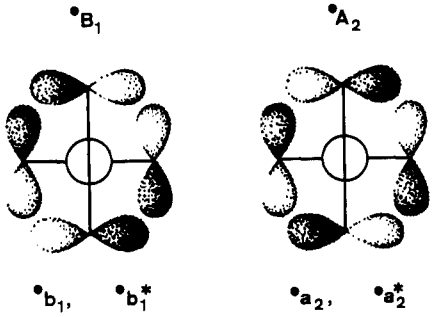

to show that to first order the split equals $\epsilon(\cdot a_2) - \epsilon(\cdot b_1) = \epsilon(\cdot a_2^*) - \epsilon(\cdot b_1^*) = -2\beta'$, if β' is the resonance integral between the spiroconnected centers 4 or 6 of one subsystem and 4 and 6 in the other.

For symmetry reasons there is no interaction between orbitals belonging to B_1 (of C_{2v}), so that $\cdot e$ and $\cdot e^*$ orbitals show the same orbital energy as b_1 and b_1^*, *i.e.*, $\epsilon(\cdot e) = \epsilon(b_1)$ and $\epsilon(\cdot e^*) = \epsilon(b_1^*)$. Finally, going from II to I, the position of the level pertaining to the lone pairs will not be changed. These considerations yield the orbital diagram shown on the right side of Figure 4.

The selection rules for electronic transitions between orbitals of a D_{2d} system are

$\cdot A_2 \longleftrightarrow \cdot A_2$ and $\cdot B_1 \longleftrightarrow \cdot B_1$, forbidden

$\cdot E \longleftrightarrow \cdot E$ and $\cdot A_2 \longleftrightarrow \cdot B_1$, allowed, z polarized

$\cdot A_2 \longleftrightarrow \cdot E$ and $\cdot B_1 \longleftrightarrow \cdot E$, allowed, x,y polarized

It follows that only the transitions indicated in Figure 4 will give rise to observable bands in the electronic spectrum, and that of these only the short-wave $\pi^* \leftarrow \pi$

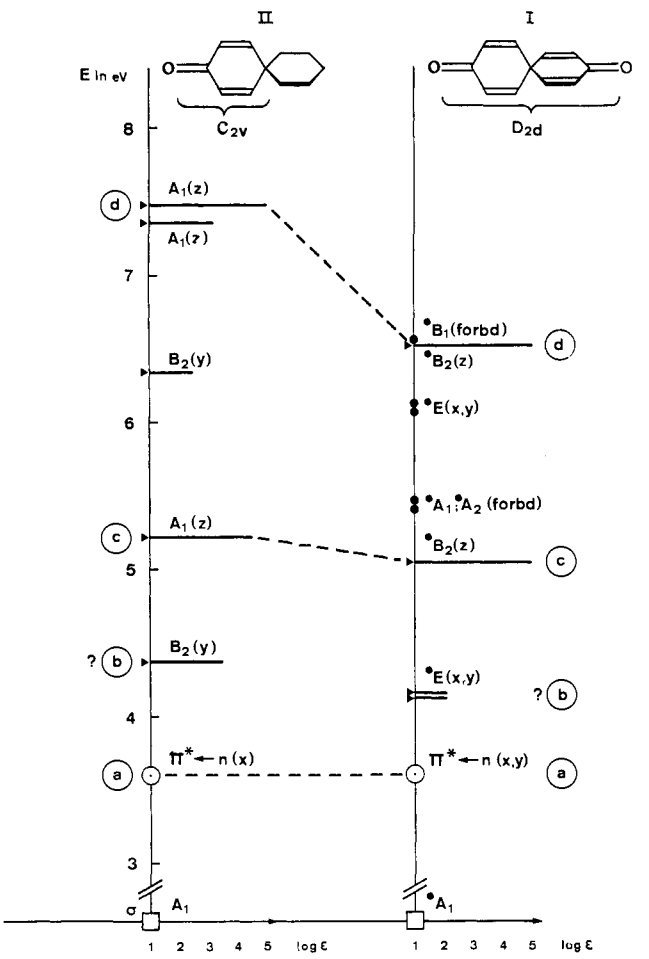

Figure 5. Computed Platt diagrams for the systems I (right) and II (left). Letters in circles refer to the features of the electronic spectra shown in Figures 1 and 2. The levels for the $\pi^* \leftarrow$ n transitions correspond to the experimental values.

transition is expected on the basis of our model to be shifted toward longer wavelengths as a consequence of spiroconjugation between the two dienone subsystems. Neglecting again any deviation from the assumed value $\alpha_O = \alpha + \beta$ for the oxygen Coulomb integral, we obtain with reference to (3)

$$E(\cdot e^* \longleftarrow n) = E(b_1^* \longleftarrow n) = -1.193\beta$$

$$E(\cdot e^* \longleftarrow \cdot e) = E(b_1^* \longleftarrow b_1) = -1.543\beta$$

$$E(\cdot b_1^* \longleftarrow \cdot a_2^*) = E(a_2^* \longleftarrow a_2) + 2\beta' = -2.400\beta + 2\beta'$$

From the observed shift $\Delta\tilde{\nu} = -7400$ cm^{-1} of the second $\pi^* \leftarrow \pi$ band on spiroconjugation, we deduce that $\beta' \approx -4000$ cm^{-1} or $\beta' \approx \beta/6$. This is only half the size of the value proposed for this quantity by Simmons and Fukunaga.[2a]

Discussion

The simple analysis given in the two previous paragraphs explains the relative electron-spectroscopic behavior of I and II, *i.e.*, the lack of change in the long-wave part of the spectrum (bands a and c) when the two dienone subsystems are spiroconnected and the pronounced bathochromic shift of the short-wave band *d*. This result demonstrates nicely the essential validity of the model proposed by Simmons and Fukunaga and

by Hoffmann, Imamura, and Zeiss,[2] when applied to our particular case.

It is interesting to examine the situation in more detail by comparing the above predictions with those obtained from a Pariser–Parr–Pople CI calculation. Under the assumptions summarized in the Appendix, one computes the results shown in Table II and in the Platt diagram of Figure 5.

We first note that the CI calculation reproduces faithfully the results of our naive orbital argument as far as the intense components of bands c and d are concerned. One of the reasons for the success of this simple HMO treatment is obvious: in view of the high symmetry of our system (I: D_{2d}) the major contribution to a given state Ψ_j is the configuration (or pair of configurations) of lowest energy belonging to the corresponding irreducible representation of the group. This is shown by the coefficient of this configuration in the particular linear combination. This will still be the case if higher energy configurations were included in the CI treatment. Hence, the low energy configurations $\psi_J^{-1}\psi_K$ themselves are good approximations to the states, and their energy is in turn primarily determined by the energy gap $\epsilon_K - \epsilon_J$ between the orbitals ψ_K and ψ_J.

The $\pi^* \leftarrow$ n transition is not included in our calculation and the corresponding level in the Platt diagram (Figure 5) is taken from the experiment. The weak transitions $\Psi_1 \leftarrow \Psi_0$ ($E \leftarrow A_1$ for I, $B_2 \leftarrow A$ for II) calculated to occur at 4.1 and 4.4 eV, respectively, and which precede the strong transition assigned to band c could be responsible for the low intensity shoulder b in the two spectra of Figures 1 and 2. If this is true, then the transition to the lowest $\pi^* \leftarrow \pi$ state of both I and II would be polarized perpendicular to the twofold axis of II or to the S_4 axis of I.

Acknowledgments. This work is part of Project No. 4651 supported by the Schweizerische Nationalfonds.

Appendix

For the Pariser–Parr–Pople treatment we have assumed idealized geometries of C_{2v} (III) and D_{2d} (I) symmetries. The bond lengths of all sp^2–sp^2 bonds have been set equal to 1.4 Å and the angles at the sp^2 centers equal to 120°. Hückel molecular orbitals ψ_J of the isoconjugate π systems were used as basis functions. In the case of I, the value $|\beta'| = |\beta|/3$, proposed by Simmons and Fukunaga was assigned to the resonance integrals between the spiroconjugating centers 4 and 6 of one subsystem with the corresponding centers in the other (*cf.* Figure 3). The nine singly excited configurations $\psi_J^{-1}\psi_K$ and the ground configuration Γ introduced into the CI treatment were based on the following set of inner π orbitals

C_{2v}: III $\psi_3(B_1)$ $\psi_2(A_2)$ $\psi_1(B_1)$ $\psi_{-1}(B_1)$ $\psi_{-2}(A_2)$ $\psi_{-3}(B_1)$

D_{2d}: I $\psi_3(\cdot A_2)\underbrace{\psi_2(\cdot E)\psi_1(\cdot E)}$ $\underbrace{\psi_{-1}(\cdot E)\psi_{-2}(\cdot E)}\psi_{-3}(\cdot B_1)$

bonding orbitals antibonding orbitals

The parameters are: $\beta = -2.371$ eV; $|\beta'| = 0.750$ eV; $\gamma_{11} = 10.959$ eV; $\gamma_{12} = 6.783$ eV; and $\gamma_{1\mu}(\mu \neq 1 \text{ or } 2) = (328.77 + R)/(30.00 + 12.34R + R^2)$ eV, if $R \leqslant 6$ Å, or $= 14.395/R$ eV, if $R > 6$ Å. R is the interatomic distance in Å. The same γ terms were used for the centers in spiroconjugation. Finally, the value $\Delta U = -2.5$ eV was used to simulate the higher electron affinity of the oxygen atomic orbital. No correction was introduced for the inductive effect of the sp^3 carbon atom at the spirocenter.